·临床研究·

胰腺神经内分泌肿瘤CT征象与SSTR2、VEGFR2及MGMT表达的关系

李璐杰，宋晨宇，周小琦，罗宴吉，冯仕庭，彭振鹏
(中山大学附属第一医院放射科,广东 广州 510080)

摘 要:【目的】探讨胰腺神经内分泌肿瘤(pNENs)的CT征象与生长抑素2型受体(SSTR2)、血管内皮生长因子2型受体(VEGFR2)及O^6-甲基鸟嘌呤-DNA甲基转移酶(O^6-methylguanine-DNA-methyltransferse,MGMT)表达的关系。【方法】收集2010年1月至2020年11月本机构经术后病理证实为pNENs 86例,所有患者术前均行增强CT检查,术后行SSTR2、VEGFR2、MGMT免疫组化检查。回顾性分析pNENs的CT特征与SSTR2、VEGFR2及MGMT表达情况的相关性,采用独立样本t检验或非参数检验及ROC曲线进行分析。【结果】SSTR2(+)组及SSTR2(-)组在性别、边界的差异有统计学意义(P<0.05),VEGFR2(+)组及VEGFR2(-)组在性别、最大径线≥20 cm、边界、强化率(动脉期、静脉期)及CT值比率(静脉期)的差异有统计学意义(P<0.05),MGMT(+)组及MGMT(-)组在最大径线≥20 cm、最大径、边界、强化率(动脉期)及CT值比率(平扫、动脉期、静脉期)的差异有统计学意义(P<0.05)。CT征象评估SSTR2、VEGFR2及MGMT阳性表达的AUC分别为0.847、0.761和0.749,灵敏度分别为87.18%,76.67%和90.48%,特异度分别为87.50%,73.91%和57.14%。【结论】CT征象联合临床特征可以反映pNENs中SSTR2、VEGFR2及MGMT的表达。

关键词:胰腺神经内分泌肿瘤;计算机断层扫描;生长抑素2型受体;血管内皮生长因子2型受体;O^6-甲基鸟嘌呤-DNA甲基转移酶

中图分类号:R445.3 **文献标志码:**A **文章编号:**1672-3554(2021)06-0892-08

DOI:10.13471/j.cnki.j.sun.yat-sen.univ(med.sci).2021.0610

Relationship of CT signs and Expression of SSTR2, VEGFR2 and MGMT in Pancreatic Neuroendocrine Neoplasms

LI Lu-jie, SONG Chen-yu, ZHOU Xiao-qi, LUO Yan-ji, FENG Shi-ting, PENG Zhen-peng
(Department of Diagnostic Radiology, The First Affiliated Hospital of Sun Yat-sen University, Guangzhou 510080, China)
Correspondence to: PENG Zhen-peng; E-mail: pengzhp@mail.sysu.edu.cn

Abstract:【Objective】To investigate the relationship between CT signs and expression of somatostatin receptor type 2 (SSTR2), vascular endothelial growth factor receptor type 2 (VEGFR2) and O^6-methylguanine-DNA-methyltransferse (MGMT) in pancreatic neuroendocrine neoplasms (pNENs).【Methods】The data of 86 pNENs patients confirmed by histopathology were retrospectively analyzed, including CT imaging and expression of SSTR2, VEGFR2 and MGMT. Their correlations were identified by independent-samples t test, non-parametric test and receiver operating characteristic (ROC) curves.【Results】Gender and tumor boundary were significantly different between SSTR2-positive and SSTR2-negative pNENs patients (P<0.05). Gender, maximum diameter ≥ 20 cm, boundary, enhancement ratio (arterial and venous phase) and CT value ratio (venous phase) were significantly different between VEGFR2-positive and VEGFR2-negative pNENs patients (P<0.05). Maximum diameter, maximum diameter ≥ 20 cm, enhancement ratio (arterial

收稿日期:2021-06-18
基金项目:国家自然科学基金(81571750);中华国际医学交流基金会2020SKY影像科研基金(Z-2014-07-2003-07)
作者简介:李璐杰,博士生,研究方向:放射诊断学,E-mail: lilj8@mail2.sysu.edu.cn;彭振鹏,通信作者,E-mail: pengzhp@mail.sysu.edu.cn

phase) and CT value ratio (plain, arterial and venous phase) were significantly different between MGMT-positive and MGMT-negative pNENs patients (P<0.05). The AUCs of CT signs assessing positive expression of SSTR2, VEGFR2 and MGMT were 0.847, 0.761 and 0.749 respectively, with sensitivity of 87.18%, 76.67% and 90.48% respectively, specificity of 87.50%, 73.91% and 57.14% respectively.【Conclusions】CT features combined with clinical manifestations can reflect expression of SSTR2, VEGFR2 and MGMT in pNENs.

Key words: pancreatic neuroendocrine neoplasms; computer tomography; somatostatin receptor type 2; vascular endothelial growth factor receptor type 2; O^6-methylguanine-DNA-methyltransferse

[J SUN Yat-sen Univ(Med Sci),2021,42(6):892-899]

胰腺神经内分泌肿瘤(pancreatic neuroendocrine neoplasms, pNENs)是一类起源于神经内分泌细胞的肿瘤,近年来发病率不断上升[1-3]。手术是其唯一的根治方式,但发生远处转移或晚期的患者往往不能手术,包括生长抑素类似物在内的药物治疗在这些患者的治疗中发挥重要作用,如何选择合适的药物进行精准治疗是临床上面临的难题。检验药物治疗靶点的表达情况有助于临床治疗决策,如生长抑素受体(somatostatin receptor, SSTR),血管内皮生长因子受体(vascular endothelial growth factor receptor, VEGFR),O^6-甲基鸟嘌呤-DNA甲基转移酶(O^6-methylguanine-DNA-methyltransferse,MGMT)等[4]。然而,这些分子标记物的检测需要以手术或穿刺等有创方式取得病理标本。计算机断层成像(computed tomography, CT)是pNENs全面评估的首选检查手段[5]。研究[6-8]表明,CT特征可以预测pNENs生物学行为,如增强CT可以预测pNENs的Ki-67指数。但目前尚无研究探讨CT特征与pNENs的SSTR2,VEGFR2,MGMT表达情况的相关性。因此,本研究主要通过分析CT征象与SSTR2、VEGFR2及MGMT表达情况的相关性,探讨利用无创的影像学方法反映这些药物治疗靶点的表达情况,为临床药物选择提供参考信息。

1　材料与方法

1.1　病例资料

收集2010年1月至2020年11月于中山大学附属第一医院经手术后病理证实为pNENs患者。纳入标准:患者在术前两周内行CT平扫加增强检查;患者在进行CT检查时(或之前)没有接受任何针对pNENs的手术或药物治疗;有SSTR2、VEGFR2或MGMT免疫组化结果。排除标准如下:其它恶性肿瘤病史;诊断为多发性内分泌腺瘤综合征;CT图像丢失或伪影较大影响分析。最终纳入86例。本回顾性研究方案经中山一院伦理委员会批准,免去回顾性收集患者的知情同意。

1.2　仪器及方法

采用64层螺旋CT扫描仪(Aquilion 64,Canon Medical Systems)对所有患者行上腹部扫描,扫描参数:管电流200 mAs,管电压120 kVp,层厚0.5 mm,层间隔0.5 mm。平扫后,以3 mL/s的速度通过高压注射器静脉注射碘佛醇(恒瑞),注射剂量为1.2~1.5 mL/kg,动脉期扫描时间范围为30~42 s,静脉期扫描时间范围为58~70 s。

1.3　图像分析

由2名放射科医师(分别具有5年和10年以上阅片经验)进行独立阅片,若判断结果不一致则共同协商。原发灶定性图像特征包括:位置、最大径(在病灶最大层面测量最大直径)、性质(囊性、囊实性或实性)、有无钙化、边界(清晰或不清晰)、轮廓(类圆形、局部分叶或多结节融合)、是否累及周围血管、胰腺胰管是否扩张或截断改变、胰腺是否萎缩、淋巴结短径(小于10 mm,大于等于10 mm或淋巴结融合)、淋巴结强化是否均匀。原发灶定量图像特征包括:CT值比率(平扫)(原发灶CT值/胰腺CT值)、CT值比率(动脉期)、CT值比率(静脉期)、强化率(动脉期)[(病灶动脉期CT值-病灶平扫CT值)/(同层腹主动脉动脉期CT值-同层腹主动脉平扫CT值)]、强化率(静脉期)[(病灶静脉期CT值-病灶平扫CT值)/(同层腹主动脉静脉期CT值-同层腹主动脉平扫CT值)]。ROI选择尽可能大,并避开坏死、肉眼可见血管及钙化,如图1所示。病灶ROI面积范围为0.33~16.13 cm^2。

ROI location for CT value calculation: red, lesion; green, aorta; blue, pancreas.

图1 ROI选择

Fig. 1 ROI selection

1.4 统计方法

所有统计分析使用SPSS 22.0。SSTR2组CT值比率(动脉期)、CT值比率(静脉期),VEGFR组CT值比率(动脉期),MGMT组CT值比率(动脉期)符合正态分布,数据用均数及标准差描述,两组比较采用独立样本*t*检验;其余不符合正态分布者用*M*(P_{25}~ P_{75})描述,两组比较采用非参数检验。两组分类资料的比较,采用卡方检验或Fisher精确检验;选用二元Logistic回归(逐步向前法)筛选影响因素,采用受试者工作曲线(ROC)评价其鉴别价值。以*P*值小于0.05时认为差异有统计学意义。

2 结果

2.1 SSTR2表达情况与CT征象的相关性分析

SSTR2阳性78例(90.70%),阴性8例(9.30%;图2)。两组在性别(χ^2 =5.258, *P*=0.022)及边界是否清晰(χ^2 =8.348, *P*=0.004)差异有统计学意义;年龄、症状及肿瘤最大径等征象在两组间的差异无统计学意义(*P*>0.05;表1)。

2.2 VEGFR2表达情况与CT征象的相关性分析

VEGFR2阳性30例(56.60%),阴性23例(43.40%)。两组在性别(χ^2 =6.517, *P*=0.011)、最大径线≥20 cm(χ^2 =4.956,*P*=0.026)、边界是否清晰(χ^2 =9.407, *P*=0.002)的差异有统计学意义(表2,图3)。

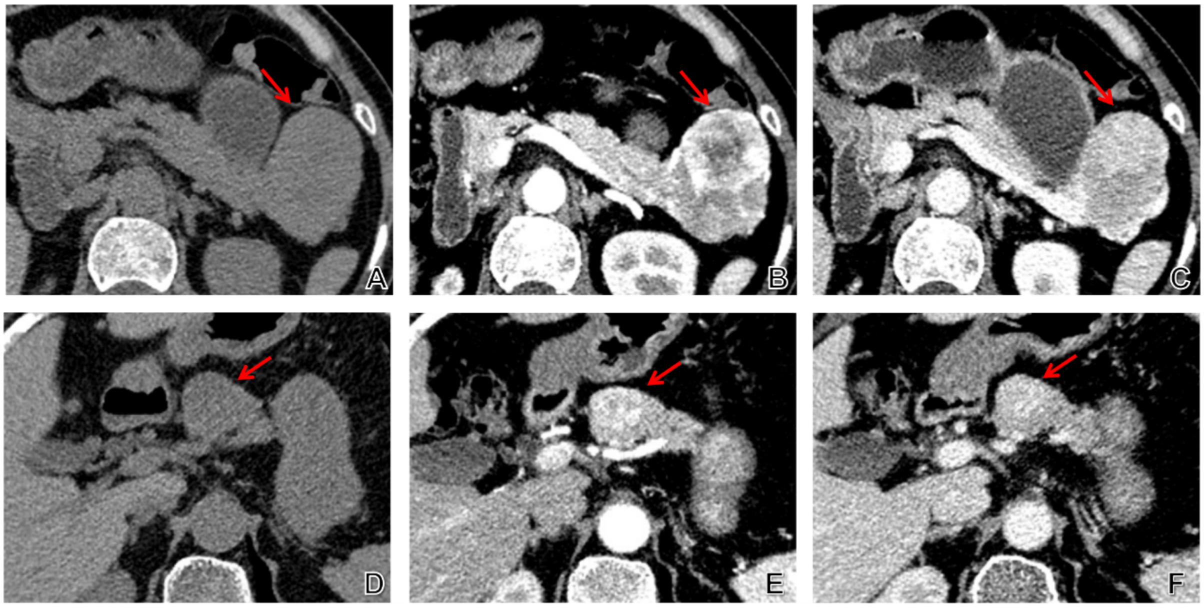

A-C: The axial CT images of a 68-year-old female patient with pNENs of SSTR2(+); A: plain scan; B: arterial phase; C: venous phase. D-F: The axial CT images of a 72-year-old female patient with pNENs of SSTR2(-); D: plain scan; E: arterial phase; F: venous phase. SSTR: somatostatin receptor.

图2 SSTR2(+)及SSTR2(-)患者CT轴位图像

Fig. 2 The axial CT images of SSTR2 positive or negative pNENs patients

表1 SSTR2与临床资料及CT征象相关性分析

Table 1 Correlation between clinical characteristics, CT signs and expression of SSTR2 [n(%)]

Clinical characteristics and CT signs	SSTR2		χ^2	P
	Positive(78)	Negative(8)		
Sex			5.258[1)]	0.022
Female	48(44.4)	1(4.6)		
Male	40(33.6)	7(3.4)		
Boundary			8.348[1)]	0.004
Clear	55(50.8)	1(5.2)		
Unclear	23(27.2)	7(2.8)		

1) Pearson Chi-square test with Yates continuity correction; SSTR: somatostatin receptor.

与VEGFR2(−)组相比，VEGFR2(+)组动脉期强化率(Z=−2.71，P<0.01)、静脉期强化率(Z=−2.584，P=0.010)、静脉期CT值比率(Z=−2.047，P=0.041)更高，差异有统计学意义。年龄、症状及其他征象在两组间的差异无统计学意义(P>0.05；表2)。

2.3 MGMT表达情况与CT征象的相关性分析

MGMT阳性63例(75.00%)，阴性21例(25.00%；图4)。两组在最大径(Z=−1.968，P=0.049)边界是否清晰(χ^2=6.481，P=0.011)、最大径线是否≥20 cm(χ^2=5.894，P=0.021)差异有统计学意义；MGMT(+)组在动脉期强化率(Z=−2.293，P=0.022)、平扫CT值比率(Z=−2.330，P=0.020)、动脉期CT值比率(t=−2.740，P=0.008)及静脉期CT值比率(Z=−2.418，P=0.016)更高，差异有统计学意义。年龄、性别、症状及其他征象在两组间的差异无统计学意义(P>0.05；表3)。

表2 VEGFR2与临床资料及CT征象相关性分析

Table 2 Correlation between clinical characteristics, CT signs and expression of VEGFR2 [M (P_{25}~ P_{75}), n(%)]

Clinical characteristics and CT signs	VEGFR2		Z/χ^2	P
	Positive(30)	Negative(23)		
Strengthening ratio (arterial phase)	0.52(0.30~0.61)	0.30(0.23~0.40)	−2.710	0.007
Strengthening ratio (venous phase)	0.65(0.51~0.78)	0.46(0.40~0.54)	−2.584	0.010
CT value ratio (venous phase)	1.14(0.96~1.45)	1.01(0.89~1.14)	−2.047	0.041
Sex			6.517	0.011
Female	21(16.4)	8(12.6)		
Male	9(13.6)	15(10.4)		
Maximum diameter ≥ 20 mm			4.956	0.026
Yes	13(17.0)	17(13.0)		
No	17(13.0)	6(10.0)		
Boundary			9.407	0.002
Clear	23(17.5)	8(13.5)		
Unclear	7(12.5)	15(9.5)		

VEGFR: svascular endothelial growth factor receptor.

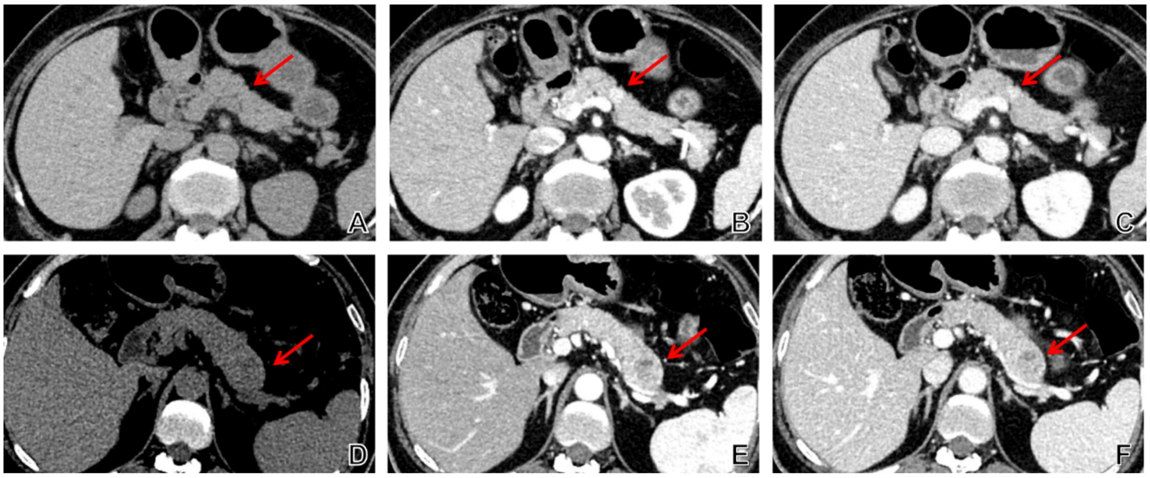

A-C: The axial CT images of a 55-year-old female patient with pNENs of VEGFR2(+); A：plain scan; B: arterial phase; C: venous phase. D-F: The axial CT images of a 57-year-old female patient with pNENs of VEGFR2(-); D: plain scan; E: arterial phase; F: venous phase. pNEN: pancreatic neuroendocrine neoplasms; VEGFRs: vascular endothelial growth factor receptor.

图3 VEGFR2(+)及VEGFR2(-)患者CT轴位图像

Fig. 3 The axial CT images of VEGFR2 positive or negative pNENs patients

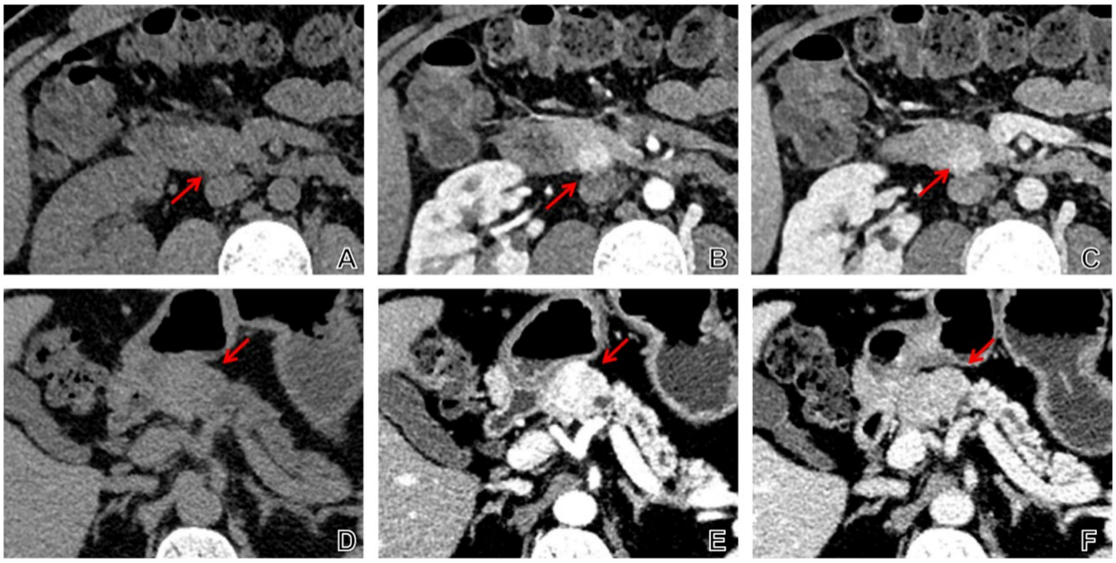

A-C: The axial CT images of a 30-year-old male patient with pNENs of MGMT(+); A：plain scan; B: arterial phase; C: venous phase. D-F: The axial CT images of a 40-year-old male patient with pNENs of MGMT(-); D: plain scan; E: arterial phase; F: venous phase. MGMT: O^6-methylguanine-DNA-methyltransferse.

图4 MGMT(+)及MGMT(-)患者CT轴位图像

Fig. 4 The axial CT images of MGMT positive or negative pNENs patients

2.4 主要影响因素与分子表达情况的ROC曲线分析

将上述有统计学差异的因素纳入二元Logistic回归分析，结果如表4所示。根据Logistic回归结果进行ROC曲线分析（图5）。利用性别及边界鉴别SSTR2表达阳性的AUC为0.847，AUC95%CI=（0.753，0.916），P<0.001；灵敏度和特异度分别为87.18%和87.50%。性别和CT值比率（静脉期）鉴别VEGFR2表达阳性的AUC为0.761，AUC95%CI=（0.624，0.867），P=0.002；灵敏度和特异度分别为76.67%和73.91%。CT值比率（动脉期）和边界鉴别MGMT表达阳性的AUC为0.749，AUC95%CI（0.643，0.838），P<0.001；灵敏度和特异度分别为90.48%和57.14%。

表3　MGMT与临床资料及CT征象相关性分析

Table 3　Correlation between clinical characteristics, CT signs and expression of MGMT

[$(\bar{x} \pm s)$, $M(P_{25}\sim P_{75})$, $n(\%)$]

Clinical characteristics and CT signs	MGMT		$Z/t/\chi^2$	P
	Positive(63)	Negative(21)		
Maximum diameter/mm	20.00(14.30~51.30)	42.00(23.80~65.50)	−1.968	0.049
Strengthening ratio (arterial phase)	0.43(0.31~0.61)	0.30(0.22~0.44)	−2.293	0.022
CT value ratio (plain)	0.80(0.64~0.99)	0.92(0.81~1.15)	−2.330	0.020
CT value ratio (arterial phase)	1.25±0.38	1.00±0.28	−2.740	0.008
CT value ratio (venous phase)	1.15(1.00~1.38)	0.97(0.83~1.15)	−2.418	0.016
Maximum diameter≥20 mm			5.894	0.021
Yes	32(36.8)	17(12.3)		
No	31(26.3)	4(8.8)		
Boundary			6.481	0.011
Clear	41(36.0)	7(12.0)		
Unclear	22(27.0)	14(9.0)		

MGMT: O^6-methylguanine-DNA-methyltransferse.

表4　多因素Logistic回归分析结果

Table 4　Results of multivariate logistic regression analysis

Variables	b	S_b	Wald χ^2	P	$\widehat{OR}$	OR95%CI
SSTR2						
Boundary	−2.593	1.118	5.382	0.020	13.367	(1.495, 119.491)
Sex	−2.139	1.126	3.607	0.058	8.488	(0.934, 77.150)
Constant	5.291	1.370	14.923	<0.001	−	−
VEGFR2						
Sex	−1.856	0.667	7.733	0.005	6.395	(1.729, 23.649)
CT value ratio (venous phase)	2.603	1.135	5.262	0.022	13.511	(1.461, 124.963)
Constant	−1.759	1.232	2.038	0.153	−	−
MGMT						
Boundary	−1.219	0.554	4.841	0.028	3.384	(1.142, 10.027)
CT value ratio (arterial phase)	1.935	0.837	5.342	0.021	6.926	(1.342, 35.741)
Constant	−0.440	0.981	0.201	0.654	−	−

SSTR: somatostatin receptor; VEGFR: svascular endothelial growth factor receptor; MGMT: O^6-methylguanine-DNA-methyltransferse.

3　讨 论

pNENs的影像学表现与生物学行为密切相关。我们先前的研究表明，pNENs的影像学表现可以预测肿瘤的病理分级[6]。在本研究中，我们探讨了pNENs的CT特征与SSTR2、VEGFR2及MGMT表达情况的关系。

SSTR包含5种亚型（SSTR1-SSTR5），大多数pNENs特征性地表现为细胞膜上大量的SSTR，尤其是SSTR2[9]。基于此，SSTR2在pNENs的诊断和治疗中都扮演了重要的角色。在本组研究中，有90.70%表达SSTR2阳性，与既往研究结果相仿[10]。

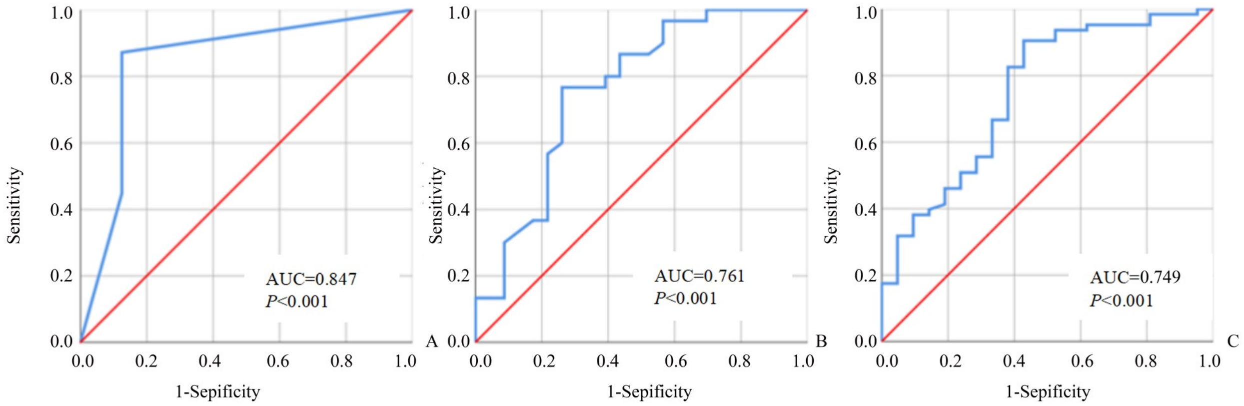

A: ROC curve of the positive expression of SSTR2 predicted by sex and boundary. B: ROC curve of the positive expression of VEGFR2 predicted by sex and CT value ratio (venous phase). C: ROC curve of the positive expression of MGMT predicted by boundary and CT value ratio (arterial phase).

图5　ROC曲线分析

Fig. 5　ROC curves

本研究发现SSTR2阳性的pNENs表现出更清楚的边界,且女性患者更多。既往研究表明,SSTR低表达可能提示肿瘤分化不良[11]。因此,SSTR阴性多为分化差的pNENs,更易出现边界不清[12]。另外,有研究表明雌激素可以上调SSTR2的表达[13],这可能解释了为什么女性患者SSTR2阳性率更高。

VEGF已证实在pNENs中与微血管密度和肿瘤进展相关[14]。我们的研究结果显示,VEGFR2阳性的病灶血供更为丰富,这可以通过VEGFR促进微血管生成的功能得到解释。而VEGFR2阳性组的肿瘤径线较小,可能与血供丰富的肿瘤早期更易被发现有关。既往研究显示,雌激素可以上调子宫肌层[15]、乳腺癌[16]等组织中VEGFR2的表达,我们推测这可能与本研究结果中VEGFR2阳性组女性更多有关,但在pNENs中尚未见有关报道,还需进一步研究加以验证。另外,有研究报道NENs中VEGFR2的表达水平与PD-1的表达水平显著相关[17],这提示我们在检查中发现病灶具有血供丰富的特点时,联合使用VEGFR抑制剂和免疫治疗可能有较好的效果。在疾病监测方面,CT可以作为一种无创的方式,动态评估VEGFR的变化,以对药物治疗方案的调整提供及时的帮助[18]。

MGMT是一种DNA修复酶,可以修复DNA的烷基化损伤。在pNENs中,替莫唑胺是一线化疗药物,而其治疗反应与MGMT的表达密切相关[19-20]。因此,MGMT的表达对预测烷化剂的疗效很重要。我们的研究结果显示MGMT(+)组强化率及CT值比率更高、直径更小、边界更清,且边界及CT值比率(动脉期)联合预测MGMT表达的灵敏度达90.48%。这些结果提示MGMT(+)组的病灶血供更为丰富。丰富的血供也可以解释为何MGMT(+)的病灶直径更小,因为血供丰富而使得病灶易于早期被发现。

综上所述,CT征象在反映pNENs中SSTR2,VEGFR2及MGMT的表达情况方面具有潜在的临床价值,这为辅助临床精准制定药物治疗方案提供了重要的参考信息。

参考文献

[1] Halfdanarson TR, Rabe KG, Rubin J, et al. Pancreatic neuroendocrine tumors (PNETs): incidence, prognosis and recent trend toward improved survival [J]. Ann Oncol, 2008, 19(10): 1727-1733.

[2] Dasari A, Shen C, Halperin D, et al. Trends in the incidence, prevalence, and survival outcomes in patients with neuroendocrine tumors in the United States[J]. Jama Oncol, 2017, 3(10): 1335-1342.

[3] Tai WM, Tan SH, Tan DMY, et al. Clinicopathologic characteristics and survival of patients with gastroenteropancreatic neuroendocrine neoplasm in a multi-ethnic Asian institution [J]. Neuroendocrinology, 2019, 108

(4): 265-277.

[4] Megdanova-Chipeva VG, Lamarca A, Backen A, et al. Systemic treatment selection for patients with advanced pancreatic neuroendocrine tumours (PanNETs) [J]. Cancers, 2020, 12(7): 1988.

[5] 中华医学会肿瘤学分会胰腺癌学组(筹). 胰腺神经内分泌肿瘤诊治专家共识[J]. 中华肿瘤杂志, 2014, 36(9): 717-720.
Pancreatic Cancer Group (preparatory), Society of O. Consensus statement on the diagnosis and treatment of pancreatic endocrine tumors[J]. Chin J Oncol, 2014, 36(9): 717-720.

[6] Luo Y, Dong Z, Chen J, et al. Pancreatic neuroendocrine tumours: correlation between MSCT features and pathological classification [J]. Eur Radiol, 2014, 24 (11): 2945-2952.

[7] Guo C, Zhuge X, Wang Z, et al. Textural analysis on contrast-enhanced CT in pancreatic neuroendocrine neoplasms: association with WHO grade [J]. Abdom Radiol (NY), 2019, 44(2): 576-585.

[8] 田瑞清, 侯宝华, 王慧玲, 等. 胰腺神经内分泌肿瘤49例诊治分析[J]. 广东医学, 2014, 35(3): 379-381.
Tian RQ, Hou BH, Wang HL, et al. Diagnosis and treatment of 49 cases of pancreatic neuroendocrine tumors [J]. Guangdong Med J, 2014, 35 (3): 379-381.

[9] de Herder W W, Hofland L J, van der Lely A J, et al. Somatostatin receptors in gastroentero-pancreatic neuroendocrine tumours[J]. Endocr-Relat Cancer, 2003, 10(4): 451-458.

[10] Hofland J, Kaltsas G, de Herder WW. Advances in the diagnosis and management of well-differentiated neuroendocrine neoplasms[J]. Endocr Rev, 2020, 41 (2): 371-403.

[11] Kayani I, Bomanji JB, Groves A, et al. Functional imaging of neuroendocrine tumors with combined PET/CT using 68Ga-DOTATATE (DOTA-DPhe1, Tyr3-octreotate) and 18F-FDG [J]. Cancer-Am Cancer Soc, 2008, 112(11): 2447-2455.

[12] Ciaravino V, De Robertis R, Tinazzi Martini P, et al. Imaging presentation of pancreatic neuroendocrine neoplasms [J]. Insights Imaging, 2018, 9 (6): 943-953.

[13] Kimura N, Takamatsu N, Yaoita Y, et al. Identification of transcriptional regulatory elements in the human somatostatin receptor sst2 promoter and regions including estrogen response element half-site for estrogen activation[J]. J Mol Endocrinol, 2008, 40(2): 75-91.

[14] Terris B, Scoazec JY, Rubbia L, et al. Expression of vascular endothelial growth factor in digestive neuroendocrine tumours[J]. Histopathology, 1998, 32(2): 133-138.

[15] Trenti A, Tedesco S, Boscaro C, et al. Estrogen, angiogenesis, immunity and cell metabolism: solving the puzzle[J]. Int J Mol Sci, 2018, 19(3): 859.

[16] Garvin S, Nilsson UW, Dabrosin C. Effects of oestradiol and tamoxifen on VEGF, soluble VEGFR-1, and VEGFR-2 in breast cancer and endothelial cells[J]. 2005, 93(9): 1005-1010.

[17] Bösch F, Altendorf-Hofmann A, Jacob S, et al. Distinct expression patterns of vegfr 1-3 in gastroentero-pancreatic neuroendocrine neoplasms: supporting clinical relevance, but not a prognostic factor[J]. J Clin Med, 2020, 9(10): 3368.

[18] Ng CS, Wei W, Duran C, et al. CT perfusion in normal liver and liver metastases from neuroendocrine tumors treated with targeted antivascular agents[J]. Abdom Radiol (NY), 2018, 43(7): 1661-1669.

[19] Lemelin A, Barritault M, Hervieu V, et al. O^6-methylguanine-DNA methyltransferase (MGMT) status in neuroendocrine tumors: a randomized phase II study (MGMT-NET)[J]. Digest Liver Dis, 2019, 51(4): 595-599.

[20] Campana D, Walter T, Pusceddu S, et al. Correlation between MGMT promoter methylation and response to temozolomide-based therapy in neuroendocrine neoplasms: an observational retrospective multicenter study[J]. Endocrine, 2018, 60(3): 490-498.

（编辑　余　菁）